Electronic structure and optical properties of PbI_2†

I. Ch. Schlüter and M. Schlüter

Laboratoire de physique appliqueé EPF, Lausanne, Switzerland
Department of Physics, University of California, Berkeley, California 94720
Inorganic Materials Research Division, Lawrence Berkeley Laboratory, University of California, Berkeley, California 94720
(Received 11 October 1973)

The electronic structure of the layer compound PbI_2 is calculated within the framework of the empirical pseudopotential method. Spin-orbit interactions were necessarily included to explain experimental reflectivity measurements. Using the pseudo-wave-functions, electronic charge densities were computed. They are discussed in terms of the nature of the chemical bonding for PbI_2.

I. INTRODUCTION

Lead iodide is an anisotropic semiconductor which crystallizes in the CdI_2 type of layer structure.[1] Its optical properties have been studied in a number of experiments.[2-10] Early optical measurements revealed the existence of a hydrogenic exciton series associated with the absorption edge.[2] The exciton lines could reasonably be fitted to a Rydberg series $E_n = E_{gap} - R/n^2$ with $E_{gap} = 2.552$ eV and $R = 0.127$ eV except for the $n = 1$ line, which was shifted to higher energies by about 0.07 eV.[3] Several explanations of this anomaly have since been given.[2,9] More recent results[10] suggest that both the electron and hole functions which form the exciton wave function mainly originate from Pb orbitals ("cationic exciton"). The anomaly of the $n = 1$ exciton line could then be explained in terms of a repulsive central-cell correction due to orthogonality requirements.[10] In addition, absorption and reflectivity measurements have been performed above the fundamental absorption edge; these show a complex structure up to 10 eV and give evidence of several metastable exciton states.[7,8]

Because until recently no band-structure calculations were available, several models for the band structure were proposed.[5,8] The first quantitative band-structure calculation was carried out in the semiempirical tight-binding scheme.[11] Though these calculations gave some insight into the electronic structure of PbI_2, they were not able to explain all optical experiments. Tight-binding calculations are known to give inaccurate descriptions of conduction bands, so that the discrepancy between these calculations and experiment is not surprising.

The aim of this paper is to present a more reliable band-structure calculation for PbI_2 which gives many of the answers to the puzzling experimental results. To do so, we have chosen the empirical pseudopotential method (EPM), which in the past has been successfully used for band calculations of layered compounds.[12-14] The basic concept is first to associate a pseudopotential with each ion core independent of its chemical state and then to vary slightly the different form factors to fit the optical data of the actual compound.

In Sec. II we discuss the crystal structure of PbI_2 and give some important group-theoretical results. The method of calculations of the band structure and of the charge densities, as well as the calculations of optical spectra, are described in Sec. III. In Sec. IV the results of the calculations are compared to experiment. The calculated optical structure is discussed in terms of interband transitions. The influence of spin-orbit interaction on the band structure and on the transition matrix elements is outlined. The electronic charge densities are calculated for all valence bands and the first three conduction bands; they are discussed in terms of chemical bonding in PbI_2.

II. CRYSTAL STRUCTURE AND GROUP THEORY

The $2H$ polytype of lead iodide belongs to the CdI_2 type of structure. Its hexagonal unit cell, which is defined by the three basis vectors

$$t_1 = \begin{pmatrix} a/2\sqrt{3} \\ -a/2 \\ 0 \end{pmatrix}, \quad t_2 = \begin{pmatrix} 0 \\ a \\ 0 \end{pmatrix}, \quad t_3 = \begin{pmatrix} 0 \\ 0 \\ C \end{pmatrix},$$

with the lattice constants $a = 4.56$ Å, and $c = 6.98$ Å,[1] contains a single molecule. The atoms are in the following positions of $D_{3d}^3(C\bar{3}m)$: Pb: (0, 0, 0); I: $(\frac{1}{3}, \frac{2}{3}, u)$; $(\frac{2}{3}, \frac{1}{3}, -u)$, with $u \simeq 0.265$.[1] The structure is characterized by an octahedral coordination of the cations and by anion-anion contacts along certain directions, which allows the structure to be viewed as layerlike. A perspective view of the atomic arrangement is given in Fig. 1. With $u = 0.265$ and $c/a = 1.53$ the iodine atoms are located in almost perfect hexagonal close packing ($u = 0.25$, $c/a = 1.63$). The lead-to-iodine distance is 3.22 Å and the interlayer iodine-iodine separa-

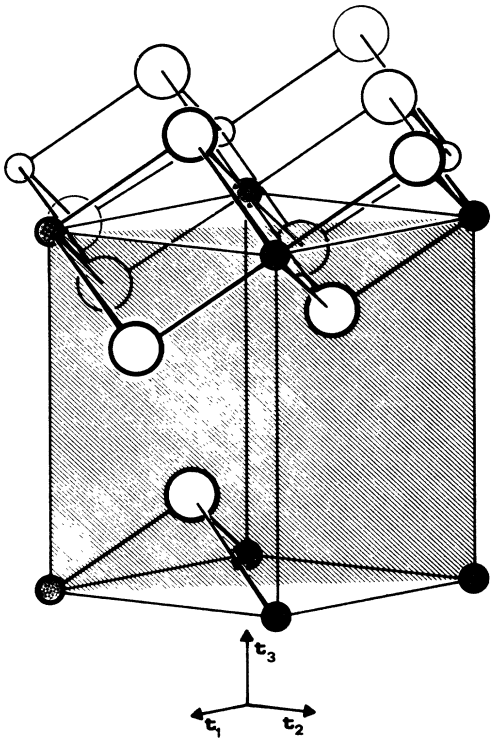

FIG. 1. Perspective view of the atomic positions in PbI_2. The large circles mark the iodine atoms, the small shaded circles represent the lead atoms. The (110) plane is indicated.

tion is 4.21 Å. These distances are about 5% smaller than the sums of the corresponding ionic radii; from this standpoint the crystal can be viewed as hexagonal close packing of iodine ions with the small lead ions intercalcated between alternate layers of iodine.

A detailed discussion of the symmorphic crystal space group D_{3d}^3 is given in Ref. 13. For convenience we repeat, here, only some of these results. In addition to the primitive lattice translations, there exist 12 more point-group operations which leave the crystal structure unchanged. They are the identity operator E, two threefold rotations ($2C_3$) about the $\vec{c}$ axis, three twofold rotations ($3C_2'$) about axes in a plane perpendicular to $\vec{c}$ and with an angle of 120° to each other and six more operations, which can be obtained from the six operations cited above by multiplying them with the inversion operator i. The first Brillouin zone of $2H$-PbI_2 is a hexagonal prism which is shown in Fig. 2. Since there are only 12 point-group operations, the irreducible part is $\frac{1}{12}$ of the zone and any full-k-space integration has to be carried out over this volume. Symmetry points and symmetry lines, as indicated in Fig. 2, need only to be considered in the usual $\frac{1}{24}$ of the Brillouin zone, as one readily can verify by applying to them all point-group operations together with appropriate lattice translations. This property which also holds for some symmetry planes not especially marked in Fig. 2, is of importance whenever Brillouin-zone integrals like charge densities are calculated by use of some representative $\vec{k}$ points,[15,16] as it will be done in Sec. III. The small groups associated with symmetry points and symmetry lines of the Brillouin zone are discussed in detail in Ref. 13. Since we will discuss in Sec. IV optical transitions at the band edge of PbI_2 and since this band edge appears at the symmetry point A, we only report here the selection rules for optical transitions of this point. Because of the uniaxial symmetry of PbI_2 the selection rules are different for incident light polarized along and perpendicular to the $\vec{c}$ axis. The allowed transitions between states belonging to the single group and to the double group of point A are summarized in Table I.

III. CALCULATIONS

The EPM is used in the present calculation. The final choice of form factors is determined by fitting them to experimental data. This approach is well established as a framework for the study of semiconductors.[17] In the following we give a brief exposition of the pseudopotential formalism as it is used in this work. The starting point is a pseudo-Hamiltonian $H_{ps} = -\Delta + V_{ps}(r)$ which can be expanded in the reciprocal lattice

$$V_{ps}(\vec{r}) = \sum_{\vec{G}} V_{ps}(\vec{G})\, e^{i\vec{G}\cdot\vec{r}}, \tag{1}$$

where $\vec{G}$ is a reciprocal lattice vector and

$$V_{ps}(\vec{G}) = \frac{1}{L} \sum_{j=1}^{L} S_j(\vec{G})\, V_j(|\vec{G}|),$$

$$S_j(\vec{G}) = e^{-i\vec{G}\cdot\vec{u}_j} \tag{2}$$

$$V_j(|\vec{G}|) = \frac{L}{\Omega_0} \int V_{ps}^j(|\vec{r}|)\, e^{-i\vec{G}\cdot\vec{r}}\, d\vec{r}\,.$$

The index j runs over all atoms in the crystal unit

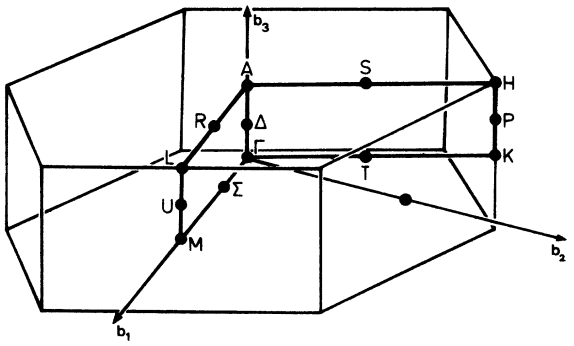

FIG. 2. First Brillouin zone of PbI_2. Several high-symmetry points and lines are indicated.

TABLE I. Allowed dipole transitions between states belonging to the single group and to the double group of point A of PbI_2. The extra representations $A_5^{\pm}$ and A_5^{-} are degenerate by time-reversal symmetry with $A_6^{\pm}$ and A_6^{-}, respectively.

A	$A_1^{\pm}$	$A_2^{\pm}$	$A_3^{\pm}$	$A_4^{\pm}$	$A_5^{\pm}$	$A_6^{\pm}$
z	$A_2^{\mp}$	$A_1^{\mp}$	$A_3^{\mp}$	$A_4^{\mp}$	$A_6^{\mp}$	$A_5^{\mp}$
xy	$A_3^{\mp}$	$A_3^{\mp}$	$A_1^{\mp}, A_2^{\mp}, A_3^{\mp}$	$A_4^{\mp}, A_5^{\mp}, A_6^{\mp}$	$A_4^{\mp}$	$A_4^{\mp}$

cell with volume Ω_0; their positions are given by the vectors $\vec{u}_j$. The potential $V_j(|\vec{G}|)$ is the Fourier transform of the pseudopotential $V_{ps}^j(|\vec{r}|)$ which is assumed to be spherical about each atom j. Note that the different form factors are normalized to the same average atomic volume Ω_0/L. Because of the anisotropy of the reciprocal lattice there is a large number of $V_j(|\vec{G}|)$ which have to be taken into account. The different discrete values were therefore computed from analytic functions of the form

$$V_j(q) = a_{j1}(q^2 - a_{j2})/(e^{-a_{j3}(q^2-a_{j4})} + 1), \tag{3}$$

where the a_{ji} are parameters defining the atomic pseudopotentials. The pseudo-Hamiltonian was then diagonalized in basis of plane waves. The band structure along symmetry lines was obtained by use of symmetrized plane waves rather than simple plane waves. This procedure has two advantages: Firstly, it considerably cuts down the computing time during the phase of adjusting the pseudopotentials; secondly, it allows a direct identification of the symmetries of the various energy bands without implicitly inspecting their wave functions. The method to construct symmetrized plane waves is described in detail in Ref. 12 and 18. The basis set of plane waves has been truncated in the following way: Plane waves with $|\vec{k}+\vec{G}| \leq E_1$ are included exactly and plane waves with $E_1 < |\vec{k}+\vec{G}| \leq E_2$ are incorporated by second-order perturbation theory.[19]

A correct description of the band structure of PbI_2 near the band edge which can afford an explanation of the optical experiments, necessitates the inclusion of relativistic effects. We thus briefly describe a way of incorporating the spin-orbit interaction into a pseudopotential secular equation as it was first proposed by Weisz[20] for white tin. Only the spin-orbit interaction is explicitly added to the pseudo-Hamiltonian since it breaks its symmetry. Other relativistic terms like the mass-velocity term and the Darwin term have the full crystal symmetry and are here thought of as being part of the empirical pseudopotential. The spin-orbit Hamiltonian is

$$H_{so} = \frac{\hbar}{4m^2c^2}\,[\vec{\nabla}\, V(\vec{r}) \times \vec{p}\,] \cdot \vec{\sigma}, \tag{4}$$

where $V(\vec{r})$ is the real crystal potential, $\vec{p}$ is the momentum operator, and $\vec{\sigma}$ is the Pauli spin operator. Since spin-orbit interaction energies are essentially determined by the potential in the core region, inclusion of Eq. (4) has to be done in the original orthogonalized-plane-wave (OPW) formulation of the pseudopotential concept. Weisz[20] has shown that the final matrix elements appearing in the pseudopotential Hamiltonian are of the form

$$H_{so,\vec{k}'s',\vec{k}s} = \sum_j \vec{\sigma}_{s's} \cdot \{\vec{\Lambda}^{pp} + \vec{\Lambda}^{cp} + \vec{\Lambda}^{pc} + \vec{\Lambda}^{cc}\}\, S_j(\vec{k} - \vec{k}'), \tag{5}$$

where $S_j(\vec{k}-\vec{k}')$ are the structure factors as defined in (2) and $\vec{\sigma}_{s's} = \langle s'|\vec{\sigma}|s\rangle$ are matrix elements in spin space between the electron-spin eigenfunctions s' and s. The four terms in the brackets denote the different contributions to the spin-orbit energy in the pseudopotential scheme. The superscripts p and c stand for plane waves and core functions, respectively. Weisz has shown that the core-core term $\vec{\Lambda}^{cc}$ is several orders of magnitude larger than the 3 terms containing plane waves, $\vec{\Lambda}^{pp}$, $\vec{\Lambda}^{cp}$ and $\vec{\Lambda}^{pc}$. In PbI_2 the ion cores consist of s-, p-, and d-like electrons. The s electrons do not contribute to the spin-orbit interaction. The valence states for which the formalism is developed are expected to be mostly s and p like; their projection onto d core states will therefore be small and changes on them due to core d-d spin-orbit interaction can be neglected. We are thus left with the contribution arising from p core electrons only. Equation (5) becomes in this particular case

$$H_{so,\vec{k}'s',\vec{k}s} = -i\vec{\sigma}_{s's} \cdot (\vec{k}' \times \vec{k}) \sum_j S_j(\vec{k}-\vec{k}')\, \lambda_j(|\vec{k}|, |\vec{k}'|), \tag{6}$$

where $\lambda_j(|\vec{k}|, |\vec{k}'|)$ is a slowly varying function of $|\vec{k}|$ and $|\vec{k}'|$ and determines the strength of the spin-orbit coupling. Instead of calculating this function by use of atomic core states we take in this paper $\lambda_j(|\vec{k}|, |\vec{k}'|) \equiv \lambda_j$ independent of $|\vec{k}|$, $|\vec{k}'|$ and consider it as atomic spin-orbit coupling parameter. Since s, s' are two-component vectors each original Hamiltonian matrix element $H_{\vec{k}',\vec{k}}$ is now replaced by a complex two-by-two matrix:

$$H_{\vec{k}'s',\vec{k}s} = k^2 \delta_{\vec{k}'\vec{k}} \delta_{s's} + \sum_j S_j(\vec{k}-\vec{k}')\,[V_j(|\vec{k}-\vec{k}'|)\,\delta_{s's} - i\vec{\sigma}_{s's} \cdot (\vec{k}' \times \vec{k})\,\lambda_j]. \tag{7}$$

This means that the Hamiltonian matrix including spin-orbit interaction has twice the size of the spin-free matrix and is complex. Since inversion is among the crystal-space-group operations each eigenvalue of the spin-orbit Hamiltonian will be at least two fold degenerate. No general formalism has been found to factorize the Hamiltonian matrix and to remove this degeneracy.

The analysis of the optical properties of PbI_2

can be done by computing the imaginary part of the frequency-dependent dielectric function $\epsilon_2(\omega)$. The calculation of $\epsilon_2(\omega)$ requires the knowledge of the band structure throughout the Brillouin zone since it has the form

$$\epsilon_2(\omega) = \frac{e^2\hbar^2}{3\pi m^2}\,\frac{1}{\omega^2}\sum_{c,v}\int d\vec{k}\,\delta(E_c(\vec{k}) - E_v(\vec{k}) - \hbar\omega) \times |\langle u_{v\vec{k}}|\,\vec{\nabla}\cdot\vec{e}\,|u_{c\vec{k}}\rangle|^2, \tag{8}$$

where $u_{v\vec{k}}$ and $u_{c\vec{k}}$ are the Bloch factors of the valence- and conduction-band wave functions and $E_v(\vec{k})$ and $E_c(\vec{k})$ are the energies of these states. $\vec{e}$ is the polarization vector of the incident light and we distinguish in PbI_2 between two polarizations, whether the light is polarized parallel ($\epsilon_2^{\parallel}$) to $\vec{c}$ or perpendicular ($\epsilon_2^{\perp}$) to $\vec{c}$. The integration over $\vec{k}$ space in Eq. (8) may be written

$$\int d\vec{k} = \int \frac{d\vec{S}}{|\vec{\nabla}_{\vec{k}}\omega(\vec{k})|}, \tag{9}$$

where $\vec{S}$ is a surface of constant interband energy $\hbar\omega = E_c - E_v$. Besides matrix element effects the structure in $\epsilon_2(\omega)$ originates from van Hove singularities,[21] at critical points where $\vec{\nabla}_{\vec{k}}(\omega) = 0$. These critical points can be classified according to symmetry as minima M_0, saddle points M_1, and M_2, and maxima M_3. The interband energies $E_c - E_v$, the dipole matrix elements $\langle u_{v\vec{k}}|\vec{\nabla}\cdot\vec{e}\,|u_{c,\vec{k}}\rangle$, and the energy gradients $\vec{\nabla}_{\vec{k}}\omega(\vec{k})$ were obtained from eigenvalues and eigenvectors of the pseudo-Hamiltonian at a number of mesh points in $\frac{1}{12}$ of the Brillouin zone. The error arising from calculating the dipole matrix elements by use of pseudo-wave-functions rather than crystal wave functions has been estimated to be of the order of 10–20%.[22] The integration was performed using the Gilat-Raubenheimer[23] scheme. In order to compare our results directly to reflectivity measurements we had to derive $R(\omega)$ from the $\epsilon_2(\omega)$ spectrum. This was done by first performing a Kramers-Kronig integration over $\epsilon_2(\omega)$ resulting in the real part $\epsilon_1(\omega)$ of the frequency-dependent dielectric constant:

$$\epsilon_1(\omega) = 1 + \frac{2}{\pi}\int_0^{\infty}\frac{\omega'\epsilon_2(\omega')}{\omega'^2 - \omega^2}\,d\omega'. \tag{10}$$

This equation means that $\epsilon_1(\omega)$ can be obtained if the $\epsilon_2(\omega)$ spectrum is known explicitly over the entire wavelength range. An analytic tail replaces the calculated $\epsilon_2(\omega)$ for higher energies. This is done to account for the high-energy transitions which are not represented in our $\epsilon_2(\omega)$ calculation considering a finite number of bands only. The tail function[24] used is

$$\beta\omega/(\omega^2 + \gamma^2)^2, \tag{11}$$

where γ is an average energy and β is determined by continuity with $\epsilon_2(\omega)$ at some cutoff energy E_c. $\epsilon_1(\omega)$ together with $\epsilon_2(\omega)$ allow the calculation of the reflectivity $R(\omega)$ for normal incidence by use of the formulas

$$\epsilon_1(\omega) = n(\omega)^2 - k(\omega)^2,$$
$$\epsilon_2(\omega) = 2n(\omega)\,k(\omega), \tag{12}$$
$$R(\omega) = \frac{[n(\omega)-1]^2 + k(\omega)^2}{[n(\omega)+1]^2 + k(\omega)^2}.$$

In order to understand the nature of bonding in PbI_2 we use the pseudo-wave-functions to calculate electronic charge distributions. For this purpose we define a "band" charge density

$$\rho_n(\vec{r}) = e\sum_{\vec{k}} |\psi_n(\vec{r},\vec{k})|^2 = e\sum_{\vec{k}}\rho_n(\vec{r},\vec{k}), \tag{13}$$

with $\vec{k}$ running over all $\vec{k}$ states in the Brillouin zone. The total charge density is then given by summing over all valence bands:

$$\rho(\vec{r}) = \sum_n \rho_n(\vec{r}) = e\sum_{\vec{k}}\rho(\vec{r},\vec{k}). \tag{14}$$

In some cases it is convenient to inspect the charge distribution for some isolated $\vec{k}$ regions only; the sum in (13) has to be modified then accordingly. Since we evaluate the wave functions $\psi_n(\vec{r},\vec{k})$ for $\vec{k}$ points within the irreducible part of the Brillouin zone only ($\frac{1}{12}$ of the zone), we have to symmetrize $\rho(\vec{r},\vec{k})$ according to the full crystal symmetry. This symmetrization procedure is completely analogous to the one necessary to obtain symmetrized basis functions of the Hamiltonian. It remains to carry out the $\vec{k}$ summation in (13) over the irreducible part of the Brillouin zone. This can either be done by sampling the $\vec{k}$ space in the usual way or, since this is very time consuming, by a very elegant method, first developed by Baldereschi[15] and Chadi and Cohen[16] which we will briefly describe here. Since $\rho(\vec{r},\vec{k})$ is a periodic function in $\vec{k}$ space it can be expanded in a Fourier series,

$$\rho(\vec{r},\vec{k}) = \rho_0(\vec{r}) + \sum_{m=1}^{\infty}\rho_m(\vec{r})e^{i\vec{k}\cdot\vec{R}_m}, \tag{15}$$

where $\vec{R}_m$ are lattice vectors in real space. From $\rho(\vec{r},\vec{k})$ we construct a function,

$$\tilde{\rho}(\vec{r},\vec{k}) = \frac{1}{M}\sum_{\{T\}}\rho(\vec{r},T\vec{k}), \tag{16}$$

which has the complete symmetry of the Bravais lattice. $\{T\}$ represents the set of M point-group operations of the Bravais lattice. We can now express $\tilde{\rho}(\vec{r},\vec{k})$ in the form

$$\tilde{\rho}(\vec{r},\vec{k}) = \rho_0(\vec{r}) + \sum_{m=1}^{\infty}\tilde{\rho}_m(\vec{r})\,A_m(\vec{k}), \tag{17}$$

with

$$A_m(\vec{k}) = \sum_{\{T\}} e^{i\vec{k}\cdot T\vec{R}_m} \quad .$$

This equation associates each $A_m(\vec{r})$ with a particular "star" of lattice vectors $\vec{R}_m$. We can carry out the sum over the Brillouin zone in (13) formally and obtain

$$\rho(\vec{r}) = \rho_0(\vec{r}) \tag{18}$$

or

$$\rho(\vec{r}) = \tilde{\rho}(\vec{r}, \vec{k}) - \sum_{m=1}^{\infty} \tilde{\rho}_m(\vec{r}) A_m(\vec{k}) .$$

In other words, the integrated charge density is equal to the (lattice-symmetric) charge density of one $\vec{k}$ point plus corrective terms. The object is now to make as many of these corrective terms $A_m(\vec{k})$ equal to zero as possible by an appropriate choice of the point $\vec{k}$. The method can be improved by use of more than one $\vec{k}$ point. Those N $\vec{k}$ points $\vec{k}_i$ and their weighing factors α_i are then determined by

$$\sum_{i=1}^{N} \alpha_i A_m(\vec{k}_i) = 0, \quad m = 1, 2, 3 \ldots$$
$$\sum_{i=1}^{N} \alpha_i = 1, \tag{19}$$

where m runs over as many "stars" as possible. Since the expansion coefficients $\tilde{\rho}_m(\vec{r})$ drop rapidly in magnitude with increasing m we should have to a good approximation,

$$\rho(\vec{r}) \approx \sum_{i=1}^{N} \alpha_i \tilde{\rho}(\vec{r}, \vec{k}_i) . \tag{20}$$

In general the solutions of (19) are not unique; a procedure to solve (19) and to find the special $\vec{k}$ points in the irreducible part of the Brillouin zone has been developed by Chadi and Cohen.[16] We only report here parts of their results for the hexagonal lattice. For $N=1$ one either has $\vec{k} = (\frac{1}{3}, 0, \frac{1}{4})$ or $\vec{k} = (0.1904, 0.1904, \frac{1}{4})$ which both satisfy (19) for the first $\{R_m\}$ "star" along z and for the first "star" in the plane $z=0$. In the present calculation we choose $N=3$ and the following three points:

$$\vec{k}_1 = (\tfrac{1}{9}, \tfrac{1}{9}, \tfrac{1}{4}), \quad \vec{k}_2 = (\tfrac{2}{9}, \tfrac{2}{9}, \tfrac{1}{4}), \quad \vec{k}_3 = (\tfrac{4}{9}, \tfrac{1}{9}, \tfrac{1}{4}),$$

with the weighting factor $\frac{1}{3}$ for each point. These three points satisfy Eqs. (19) for the first eight stars in PbI_2 except for the two stars with no x-y dependence and even z coordinates $\{R_4\} = \{^{002}_{00-2}\}$ and $\{R_{14}\} = \{^{004}_{00-4}\}$. The choice of these $\vec{k}$ points for PbI_2 has the further advantage, that all three points lie on symmetry planes. We therefore need only to consider these three points within $\frac{1}{24}$ of the Brillouin zone in spite of the fact that in PbI_2 the reduced part extends over $\frac{1}{12}$ of the Brillouin zone.

IV. RESULTS AND DISCUSSION

Among the enormous number of pseudopotential data available, at present there is only little information about lead form factors[22] and—at least to our knowledge—none at all about iodine form factors. Earlier EPM calculations on the semiconducting compound PbTe[25] successfully used form factors for Pb which did not considerably differ from the model potential values of Animalu and Heine.[26] We therefore scaled their model potential form factors by an appropriate volume factor and used it in our calculations. The Animalu-Heine model potentials are screened by a free-electron-type screening function. Replacing this screening function by a Penn-type[27] screening function, which is the more appropriate type of screening for semiconductors did not give rise to drastic changes in the band structure. In particular, the order of the first three conduction bands on the energy scale which is an important feature of the band structure, as we shall see later, did not change with the two different screening functions. The definition of a first-guess pseudopotential for iodine proved to be a far more difficult task. We finally used some of the systematic trends of pseudopotentials throughout the periodic system; i.e., we used as starting potential iodine form factors obtained by extrapolating the renormalized Animalu-Heine form factors of In, Sn, Sb, and Te. These form factors have then been varied empirically to reproduce the numerical value of the gap $E_g = 2.5$ eV and to give the right order of the conduction bands. The final pseudopotentials neglecting spin-orbit interaction are defined by the values of the parameters a_{ij} given in Table II which enter Eq. (3) together with q in reciprocal Bohr radii in order to give $V_i(q)$ in rydbergs.

The convergence of the energy eigenvalues and the wave functions was tested and found to be satisfactory if one sets $E_1 = 3$ Ry and $E_2 = 6$ Ry which corresponds to about 75 planes included exactly into the Hamiltonian matrix and to about some 150 more waves included by second-order perturbation theory. The band structure of PbI_2 calculated in this way is shown in Fig. 3. The labeling of the symmetry points and lines corresponds to that in Fig. 2. There are 18 valence electrons which

TABLE II. Empirical parameters defining the pseudopotentials of Pb and I. The values enter Eq. (3) together with q in reciprocal Bohr radii in order to give $V(q)$ in rydbergs.

	a_1	a_2	a_3	a_4
Pb	0.58	2.1	0.5	−2.0
I	6.5	1.7	0.46	−6.5

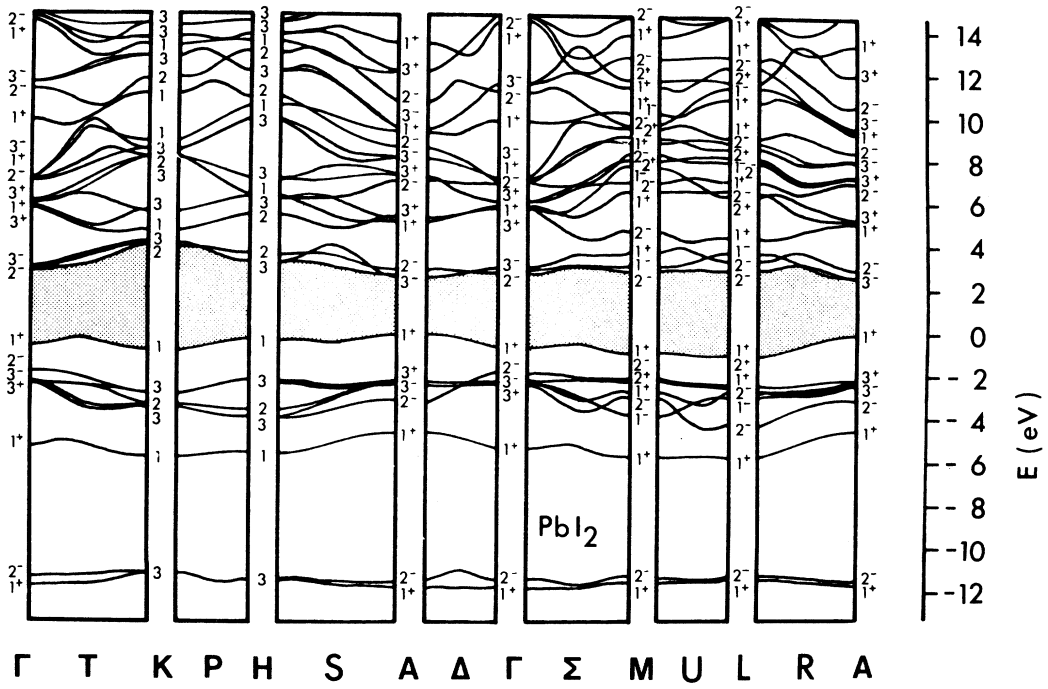

FIG. 3. Band Structure of PbI_2 along high-symmetry lines in the hexagonal Brillouin zone.

fill the first nine bands. Using the simple $8-N$ rule in its general form[28] these nine bands should essentially correspond to the iodine s and p states and to the lead s states. This contrasts, e.g., with CdI_2 or $SnSe_2$ which crystallize in the same structure but whose cation s states are essentially conduction states.[13] The lowest conduction bands in PbI_2 should be p-like lead which is confirmed by charge-density calculations as we shall see later. The smallest gap appears at the surface of the Brillouin zone at point A (which is group theoretically equivalent to point Γ) between the nondegenerate state A_1^+ and the twofold-degenerate level A_3^-. The third p-like level A_2^- appears about 0.6 eV higher in energy. Optical transitions from A_1^+ to A_3^- are allowed for light polarized perpendicular to the $\vec{c}$ axis ($E_{\perp c}$) only. This is in contrast to experiment[7,8] which shows an excitonic transition at 2.5 eV for both polarizations, though the transition is about four times stronger for $E_{\perp c}$. To explain these experimental facts we need to consider spin-orbit interaction. In fact, group-theoretical arguments show that in the double group, the band-edge exciton is visible for both polarizations: A_1^+ goes into A_4^+ and A_3^- splits into A_4^-, and the two one-dimensional states A_5^-, A_6^- which are degenerate by time-reversal symmetry; A_2^- goes into A_4^- too. Transitions from A_4^+ into A_4^- are allowed for both directions of polarization as seen from Table I.

In order to obtain quantitative results we carried out pseudopotential calculations including spin-orbit interaction as described in Sec. III. The used formalism allows to vary the strength of the spin-orbit coupling for Pb and I separately. Figure 4 shows the band structure at point A as a function of the two spin-orbit parameters λ_{Pb} and λ_I for a constant spin-free pseudopotential. Since the otherwise real Hamiltonian matrix here became complex and doubled in size we used for this calculation a lower stage of convergence, i.e., $E_1 = 2.5$ Ry and $E_2 = 5.0$ Ry which corresponds to 110 and 320 plane waves, respectively. As expected, the two lowest states have iodine s character and are thus not influenced by spin-orbit interaction. The next higher six bands mainly respond to λ_I and not to λ_{Pb}, thus indicating their predominant iodine p character. The uppermost valence band is thought to be s-like lead with some iodine p admixture and thus only slightly responds to λ_I. The lowest three conduction states reveal their p-like lead character as showing strong dependence on λ_{Pb}. As predicted by group theory the lowest conduction level A_3^- splits into A_4^- and A_5^-, A_6^-. We assume from this analysis that the uppermost valence band as well as the three lowest conduction bands are essentially lead orbitals. This assumption will later be confirmed by the charge density calculations.

Transitions at the band edge in PbI_2 are therefore "cationic" as suggested in Ref. 10. This particular situation allows us to describe the influence of spin-orbit interaction on the band gap

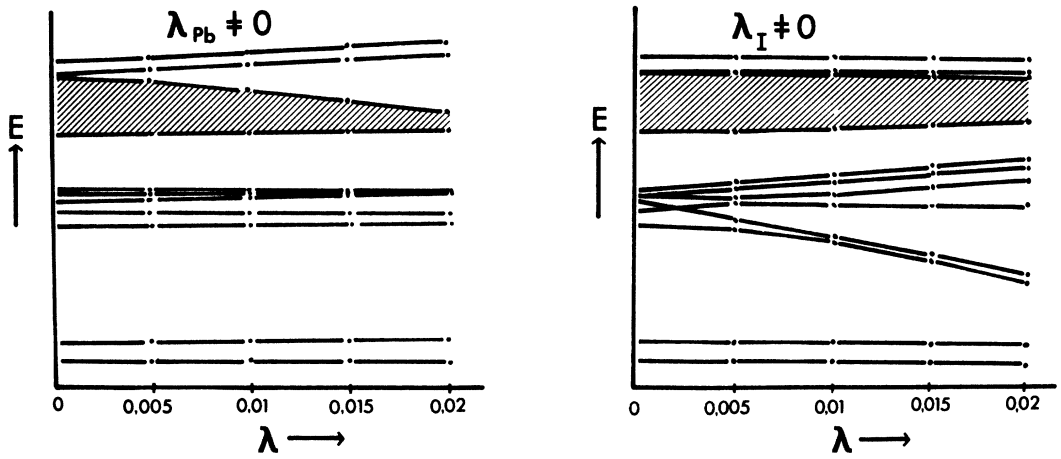

FIG. 4. Energy bands of PbI_2 at point A as a function of the spin-orbit parameters λ_{Pb} and λ_I.

in an atomiclike semiempirical model.[31] In this model we describe the PbI_2 conduction bands by atomiclike localized lead orbitals neglecting the admixture of iodine orbitals and add crystal-field and spin-orbit effects as perturbtaions. Let us define the following basis functions $|l, m_l, m_s\rangle$ with $l=1$, $m_l=-1, 0, 1$, and $m_s=\pm\frac{1}{2}$. The trigonal crystal field H_c splits the state $m_l=0$ from the states $m_l=\pm 1$ by ΔE_c:

$$\begin{aligned}&\langle 1, 0, m_s|H_c|1, 0, m_s\rangle=\Delta E_c,\\ &\langle 1, \pm 1, m_s|H_c|1, \pm 1, m_s\rangle=0.\end{aligned}\tag{21}$$

Magnitude and sign of ΔE_c are treated as empirical parameters. The spin-orbit interaction, which can be written in the form

$$H_{so}=\frac{\alpha^2}{2}\frac{1}{r}\frac{dV(r)}{dr}(\vec{L}\cdot\vec{S}),\tag{22}$$

where α is the fine-structure constant, gives rise to the following matrix elements:

$$\begin{aligned}&\langle l, m_l, \tfrac{1}{2}|H_{so}|l, m_l, \tfrac{1}{2}\rangle=m_l\lambda,\\ &\langle l, m_l+1, -\tfrac{1}{2}|H_{so}|l, m_l+1, -\tfrac{1}{2}\rangle=-(m_l+1)\lambda,\\ &\langle l, m_l, \tfrac{1}{2}|H_{so}|l, m_l+1, -\tfrac{1}{2}\rangle=[(l-m_l)(l+m_l+1)]^{1/2}\lambda,\end{aligned}\tag{23}$$

where

$$\lambda=\frac{1}{2}\int_0^\infty [R_l(\vec{r})]^2\left(\frac{\alpha^2}{2}\frac{1}{r}\frac{dV(r)}{dr}\right)r^2dr$$

and describes the strength of the spin-orbit coupling. Matrix elements of the $(\vec{L}\cdot\vec{S})$ operator are only nonzero between states of the same l and the same $m_j=m_l+m_s$. Moreover, they do not depend on the sign of m_j and we will thus be left with the following 3×3 matrix equation determining the energies:

$$\begin{pmatrix}\lambda-E & 0 & 0\\ 0 & -\lambda-E & \sqrt{2}\lambda\\ 0 & \sqrt{2}\lambda & \Delta E_c-E\end{pmatrix}\times\begin{pmatrix}|1, 1, \frac{1}{2}\rangle, & |1, -1, -\frac{1}{2}\rangle\\ |1, -1, \frac{1}{2}\rangle, & |1, 1, -\frac{1}{2}\rangle\\ |1, 0, \frac{1}{2}\rangle, & |1, 0, -\frac{1}{2}\rangle\end{pmatrix}=0.\tag{24}$$

The three eigenvalues, each twofold degenerate, are given by

$$\begin{aligned}&E_1=\lambda,\\ &E_{2,3}=\tfrac{1}{2}(\Delta E_c-\lambda)\pm(\tfrac{1}{4}\Delta E_c^2+\tfrac{5}{4}\lambda^2+\tfrac{1}{2}\Delta E_c\lambda)^{1/2}.\end{aligned}\tag{25}$$

While the eigenfunctions of E_1 are pure p_x-p_y-like and transform like A_5^-, A_6^-. The eigenfunctions of E_2, E_3 are mixtures of p_z and p_x, p_y transforming like A_4^-. We find, in particular,

$$\begin{aligned}&|E_2\rangle=[(\lambda+E_2)^2+2\lambda^2]^{-1/2}[\sqrt{2}\lambda\,|p_x, p_y\rangle+(\lambda+E_2)|p_z\rangle],\\ &|E_3\rangle=[(\lambda+E_3)^2+2\lambda^2]^{-1/2}[\sqrt{2}\lambda\,|p_x, p_y\rangle+(\lambda+E_3)|p_z\rangle].\end{aligned}\tag{26}$$

For $\lambda\to 0$, $|E_2\rangle$ becomes pure p_z-like and $|E_3\rangle$ becomes pure p_x-p_y-like. Let us now consider optical transitions from the uppermost valence band into the lowest conduction band $|E_3\rangle$. The strength of these transitions will be proportional to

$$|M_{xy}|^2=\frac{2\lambda^2}{(\lambda+E_3)^2+2\lambda^2}\quad\text{for}\quad E_{\perp c}$$

and to

$$|M_z|^2=\frac{(\lambda+E_3)^2}{(\lambda+E_3)^2+2\lambda^2}\quad\text{for}\quad E_{\parallel c}.\tag{27}$$

For $\lambda\to 0$ we correctly find the single-group selec-

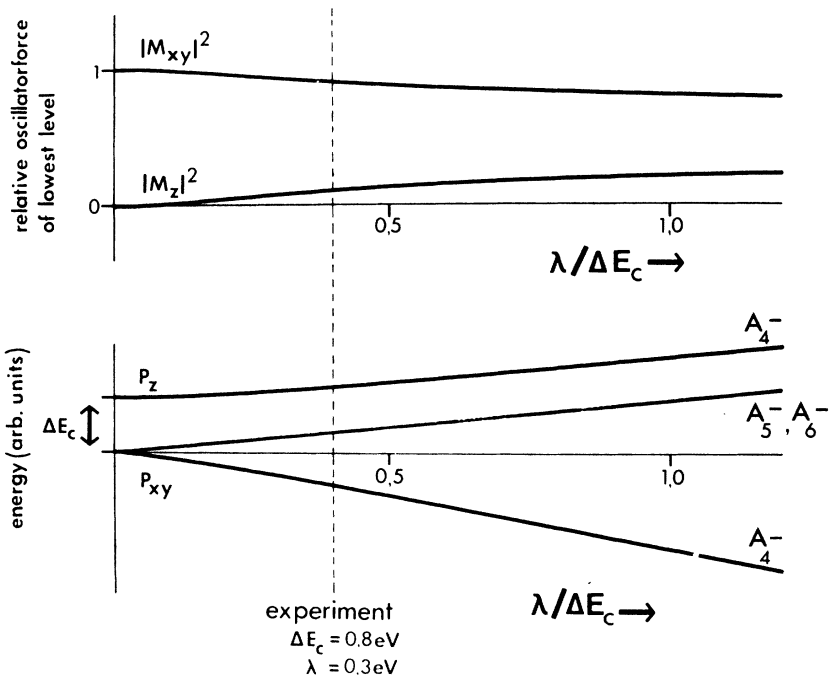

FIG. 5. Band model for point A in PbI_2. The lower plot shows the energy as a function of the normalized spin-orbit interaction $\lambda/\Delta E_c$. The upper plot indicates the variation of oscillator strength for transitions into the lower conduction band as a function of $\lambda/\Delta E_c$. The dotted line marks the experimental situation.

tion rules: $|M_{xy}|^2 = 1$ and $|M_z|^2 = 0$. Figure 5 illustrates these results: the lower plot shows the energies of the three states and the upper plot the relative oscillator strength of transitions into the lowest conduction band as a function of $\lambda/\Delta E_c$. The validity of the used model can be checked by comparing Figs. 4 and 5.

We shall now compare these results to experiment. Figure 6 thus shows the measured reflectivity of PbI_2[7] for $E_{\perp c}$ and $E_{\parallel c}$ between 2.5 and 4.5 eV. The strong excitonic resonances at the band edge are not shown in this plot; their structures are discussed in Refs. 10 and 31. As proposed in Ref. 31 we attribute the three peaks at 2.5, 3.3, and 3.9 eV to transitions from the A_4^+ valence band into the A_4^-, (A_5^-, A_6^-) and A_4^- conduction bands respectively. All three transitions seem to have excitonic character[7,31] and appear at M_0-type band edges. Because of spin-orbit coupling the transition at 2.5 eV is allowed for both polarizations of light, though the transition is about 4 times stronger for $E_{\perp c}$ than for $E_{\parallel c}$. The intermediate exciton in the continuum at 3.3 eV is only visible for $E_{\perp c}$, as we expect for the transition $A_4^+ - (A_5^-, A_6^-)$. The third exciton at 3.9 eV again is visible in both polarizations for it originates from the transition $A_4^+ - A_4^-$. The energies of these three transitions together with the observed 4:1 ratio of oscillator strengths of the lowest exciton were used to compute the parameters, $\Delta E_c = +0.8$ eV and $\lambda = 0.3$ eV of the band model which compare well with the parameters given in Ref. 31. This situation is indicated in Fig. 5 by the broken line. The p-state spin-orbit splitting $3\lambda = 0.9$ eV is somewhat smaller than that of atomic lead $3\lambda = 1.3$ eV.[30] The crystal-field splitting ΔE_c has to be positive in order to get agreement with experiment. This information was used in determining the iodine pseudopotential. At the center of the Brillouin zone (Γ) the crystal-field splitting is found to be negative. This causes the pure p_x-p_y-like state (Γ_5^-, Γ_6^-) to be the topmost state. We believe the strong peak at 4.5 eV in the $E_{\perp c}$ reflectivity to originate from transitions from the Γ_4^+ valence band into this state. The shoulders at 3.0, 3.6, and 4.3 eV which are about equally

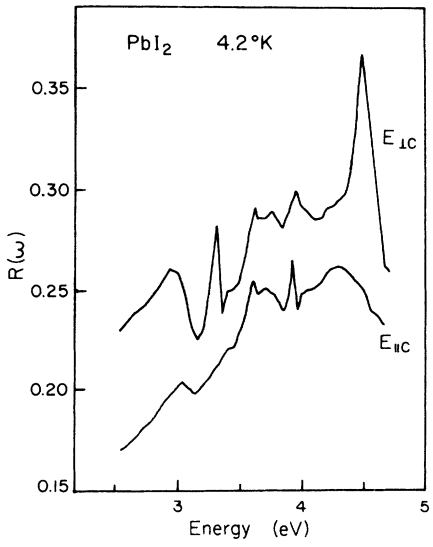

FIG. 6. Measured reflectivity of PbI_2 after Ref. 7 for polarizations $E_{\perp c}$ and $E_{\parallel c}$.

visible in both polarizations correspond to transitions from the highest valence band into the three conduction bands at generally $\vec{k}$ points within the Brillouin zone where the strong selection rules are relaxed. The fine structure[10,31,32] of the 2.5-eV band-edge exciton which is indicative for the presence of polariton effects and electron-hole exchange will be discussed in a separate paper.[29]

We showed in the last paragraph that the inclusion of spin-orbit interaction is necessary to quantitatively explain the excitonic structure of PbI_2. However, it is nevertheless of interest to compare the measured reflectivity over a wide energy range with the reflectivity derived from a band-structure calculation neglecting spin-orbit interaction. This reflectivity was computed as described in Sec. III from about 200 $\vec{k}$ points within the irreducible part of the Brillouin zone. About 25 bands up to an energy of 12 eV were included; above 10 eV the calculated dielectric function was continued by an analytic tail function [Eq. (11)] with $\gamma = 4.5$ eV. The result of this calculation together with the experimental reflectivity[8] for $E_{\perp c}$ is displayed in Fig. 7. One readily recognizes two distinct regions: structures between 2.5 and 4.5 eV originate from transitions from the isolated uppermost valence band into the lowest three conduction bands. Because of the nature of the involved bands we classify these transitions as "cationic." The structures between 4.5 and 7 eV are associated with transitions from the next deeper valence bands which are essentially iodine p-like into the p-like lead conduction bands. These anion-cation transitions allow to define an "ionic gap" $c \approx 5-6$ eV for PbI_2. The matrix elements involved in the transitions are of about equal magnitude for both regions. The experimental curve is about 0.5 eV more spread out in region 1. We believe that this difference is mainly due to spin-orbit splitting which increases the widths of the p-like lead conduction bands from 1.5 to 2.0 eV. Prominent structures in the experimental reflectivity curve can well be recognized in the calculated curve at somewhat shifted energies. The strong excitonic resonances, of course, are not reproduced by our band calculation.

In this final section we present charge-density calculations for various groups of bands in PbI_2. The purpose of doing these calculations is twofold: Firstly, we want to confirm the speculations on the cationic nature of the states near the smallest gap and, secondly, we want to obtain some information about the relative strength of ionicity and covalent bonding in PbI_2. The charge densities were calculated as described in Sec. III. Three representative $\vec{k}$ points within the irreduc-

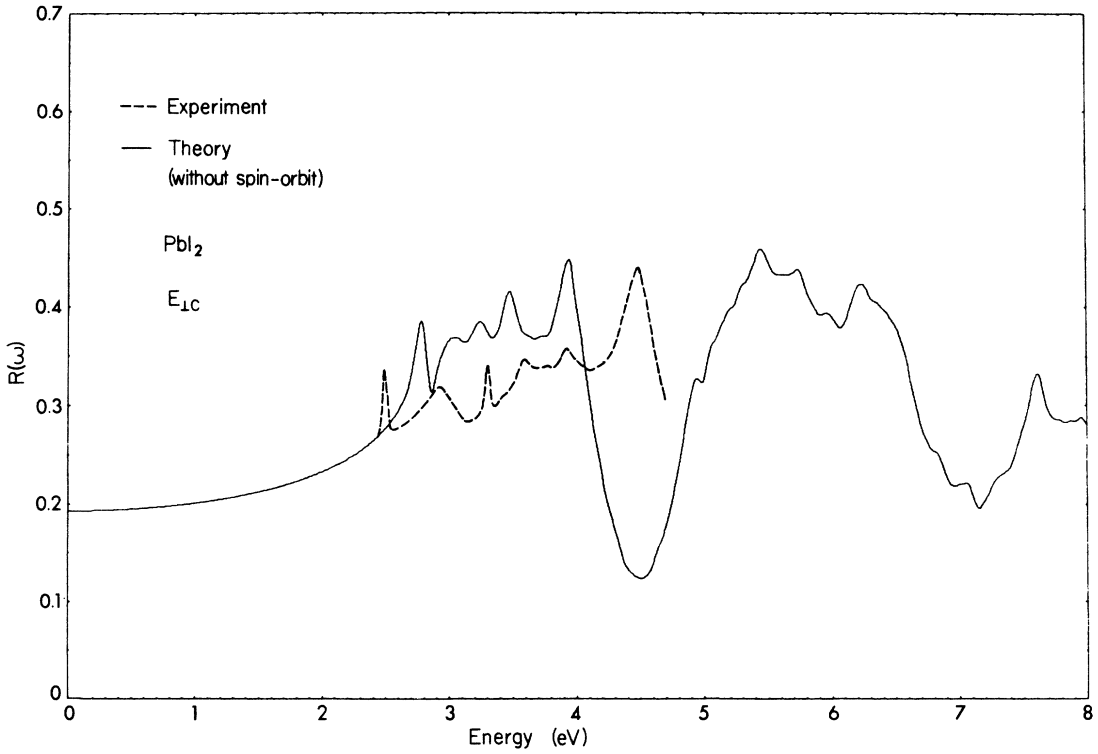

FIG. 7. Calculated reflectivity of PbI_2 for polarization $E_{\perp c}$ together with experimental data from Ref. 8.

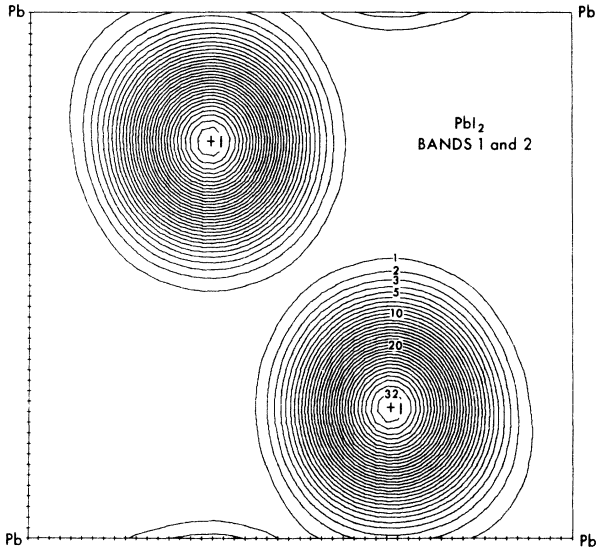

FIG. 8. Charge-density distribution of the lowest two bands in PbI_2.

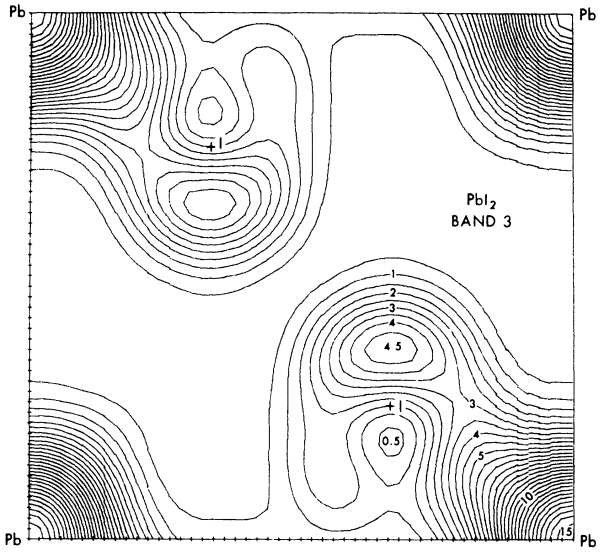

FIG. 9. Charge-density distribution of the third band in PbI_2.

ible part of the Brillouin zone were used to represent the band densities. According to earlier calculations[16] this represents the "exact" pseudocharge densities to within a few percent error. The main deviations from real charge distributions, of course, are due to the fact that our calculations are based on pseudo-wave-functions, which are not orthogonal to the core wave functions. Thus in the vicinity of the ion cores the calculated charge densities are not representative. The charge densities are displayed as contour plots in a (110) plane, depicted as the shaded area in Fig. 1. They were evaluated at 2500 points within this plane and are all normalized to two electrons per band and per unit cell volume $\Omega = \frac{1}{2}a^2c\sqrt{3}$. The charge of the lowest two bands, as shown in Fig. 8 is concentrated in the anion s states. This result, of course, is not surprising and has been found for other layer compounds[12] too. The energetic position and therefore the degree of hybridization of the anion s states depend strongly on the used iodine pseudopotential. Unfortunately there are no experimental data available at present to check these quantities. The next higher band contains already some s-like charge on the cations (see Fig. 9). This situation has also been met in GaSe, [12] where because of the existence of two nearest-neighbor Ga atoms the one band is replaced by a bonding-antibonding pair of bands. The electrons in the next group of five bands (Fig. 10) occupy mostly anion p-states. The bonding charges between Pb and I can clearly be recognized. The threefold coordination of the iodine atoms within one layer is responsible for the second charge maximum on the inside of the layers. The third maximum displayed in the (110) plane points towards the neighboring layer and might result from the repulsive interaction between the anion p states of nearest layers. Figure 11 in which the charge density of the uppermost valence band is mapped does reveal strong s-like charge around the lead atoms. There is some charge on the iodine atoms which contains p_z-like functions as well as p_x-p_y-like orbitals. A detailed analysis shows that this band mixes with iodine p_z near A and Γ and with iodine p_x, p_y near M, L, K, and H. This different mixing is, of course, compatible

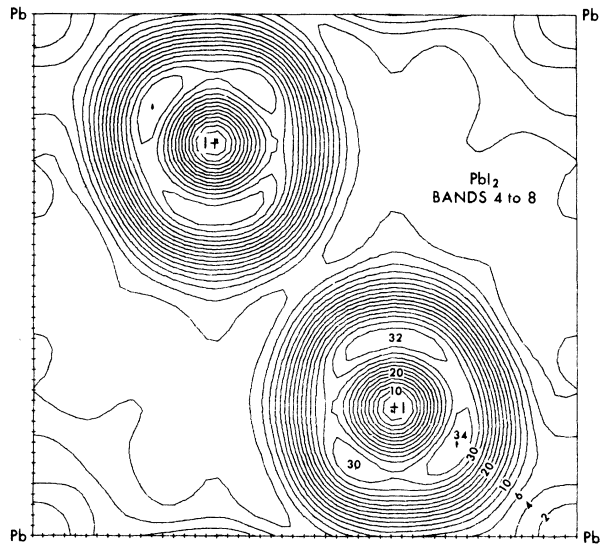

FIG. 10. Charge-density distribution of bands 4 to 8 in PbI_2.

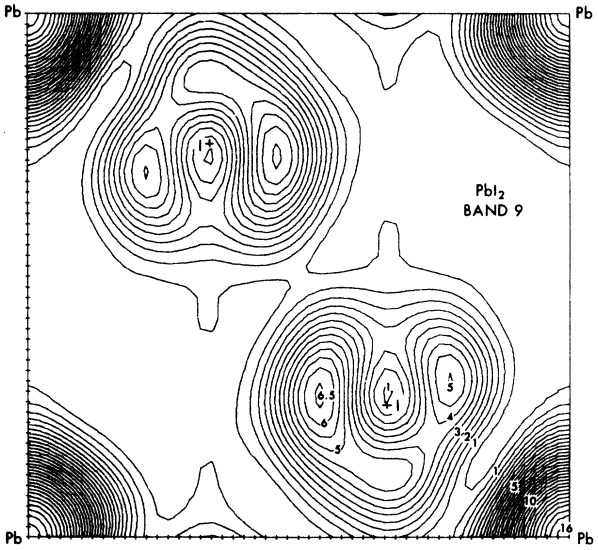

FIG. 11. Charge-density distribution of the uppermost valence band in PbI_2.

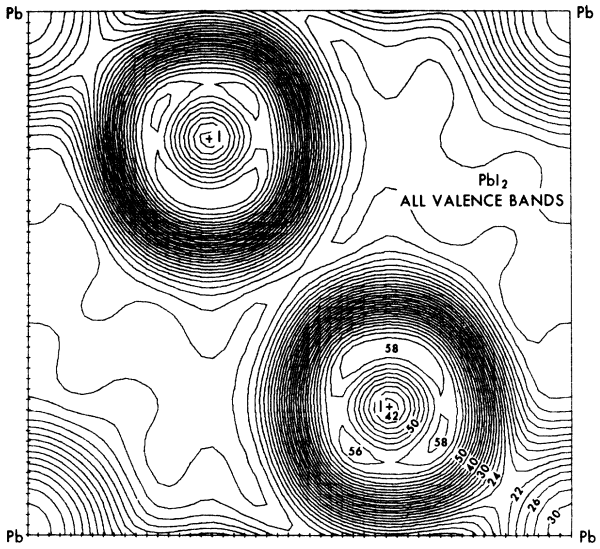

FIG. 12. Charge-density distribution of all valence bands in PbI_2.

with group-theoretical findings. It shows, however, that even a very flat band can have considerably different wave functions in different regions of $\vec{k}$ space due to interband mixing. The integrated charge of all valence electrons is shown in Fig. 12. The charge pile up at the anion and cation sites is 40 and 31, respectively. The charge between the atoms of one layer rises up to 58 and has its maximum clearly deplaced towards the more electronegative anion. We therefore conclude that there is some ionicity in the Pb-I bond. The charge distribution forms almost a closed shell for one layer. There is only little covalent binding charge recognizable between neighboring layers, indicating thus the weakness of the interlayer coupling. This result is derived for the total valence charge; at singular $\vec{k}$ point, however, some bands can reveal considerable interaction between neighboring layers, as it is, e.g., the case for the third and eighth valence bands along Γ-A. These states then have clearly three-dimensional character as seen from the dispersion of $E(\vec{k})$, but they have only little effect on the total valence charge and on the mechanical anisotropy of the crystal. In Fig. 13 the band charge of the first three conduction bands is displayed. Though there is mixing with higher bands the three bands are clearly separate on the energy scale. As expected their charge shows the pronounced lead p-like behavior. The actual asymmetry that the p_z-like charge is slightly higher than the p_x-p_y-like charge, is possible because of the trigonal crystal field. The charge on the anion sites might partially originate from iodine d levels. Similar to what has been found in other compounds, [12,13] the arrangement of charge indicates the antibonding character of the conduction bands. It follows from this discussion that optical transitions from the uppermost valence band into the lowest three conduction bands which take place in the energy range between 2.5 and 4.5 eV are mainly associated with the excitation of cationic s states into cationic p states. The large negative pressure coefficient of the band-gap exciton[33] is in agreement with these findings since s-like states are known to rise in energy much faster under pressure than do p-like states.

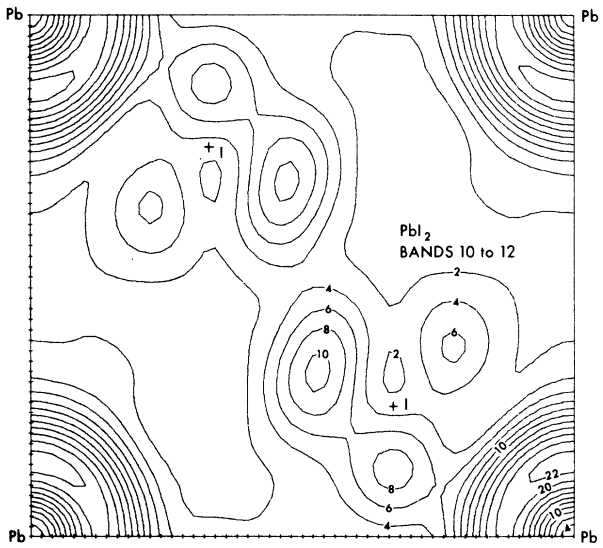

FIG. 13. Charge-density distribution of the first three conduction bands in PbI_2.

V. SUMMARY AND CONCLUSIONS

We have studied the electronic system of PbI_2 by means of the EPM. The form factors of lead were taken over from earlier calculations of PbTe, those of iodine were based on an extrapolation of the form factors of In, Sn, Sb, and Te. Spin-orbit interactions had to be considered to obtain a conduction-band structure which affords an explanation of the reflectivity measurements. In particular, the polarization dependence of the reflectivity peaks at 2.5, 3.3, and 3.9 eV can be understood in this way. Charge density calculations confirm earlier assumptions that both valence and conduction band originate essentially from lead orbitals.

ACKNOWLEDGMENTS

We are indebted to E. Mooser for many stimulating discussions and to G. Harbeke for critical comments and for making part of his measurements available to us prior to publication. We also wish to thank M. L. Cohen for helpful conversations and for a critical reading of the manuscript. Part of this work was done under the auspices of the U. S. Atomic Energy Commission.

---

†Work supported in part by the Fonds National Suisse de la Recherche Scientifique and in part by National Science Foundation Grant No. GH 35688.

[1]R. W. G. Wyckoff, *Crystal Structure*, 2nd. ed., (Interscience, New York, 1965), Vol. 1.
[2]S. Nikitine and G. Perney, C. R. Acad. Sci. (Paris) 240, 64 (1955).
[3]I. Imai, J. Phys. Chem. Solids 22, 81 (1961).
[4]M. R. Tubbs, Proc. R. Soc. Lond. A 280, 566 (1964).
[5]M. R. Tubbs, J. Phys. Chem. Solids 29, 1191 (1968).
[6]D. L. Greenaway and R. Nitsche, J. Phys. Chem. Solids 26, 445 (1965).
[7]G. Harbeke (unpublished).
[8]D. L. Greenaway and G. Harbecke, J. Phys. Soc. Jap. Suppl. 1, 151 (1965); Ch. Gähwiller and G. Harbecke, Phys. Rev. 185, 1141 (1969).
[9]G. Baldini and S. Franchi, Phys. Rev. Lett. 26, 503 (1971).
[10]G. Harbecke and E. Tosatti, Phys. Rev. Lett. 28, 1567 (1972).
[11]E. Doni, G. Grosso, and G. Spavierri, Solid State Commun. 11, 493 (1972).
[12]M. Schlüter, Nuovo Cimento B 13, 313 (1973).
[13]I. Ch. Schlüter and M. Schlüter, Phys. Status Solidi 57, 145 (1973).
[14]C. Y. Fong and M. L. Cohen, Phys. Rev. B 5, 3095 (1972).
[15]A. Baldereschi, Phys. Rev. B 7, 5212 (1973).
[16]D. J. Chadi and M. L. Cohen, Phys. Rev. B 7, 692 (1973); Phys. Rev. (to be published).
[17]See Ref. 12 and references therein.
[18]B. Renaud and M. Schlüter, Helv. Phys. Acta 45, 66 (1972).
[19]D. Brust. Phys. Rev. 134, A1337 (1964).
[20]G. Weisz, Phys. Rev. 149, 504 (1966).
[21]L. Van Hove, Phys. Rev. 89, 1189 (1953).
[22]M. L. Cohen and V. Heine, *Solid State Physics* (Academic, New York, 1970), Vol. 24.
[23]G. Gilat and L. J. Raubenheimer, Phys. Rev. 144, 390 (1966).
[24]J. P. Walter, M. L. Cohen, Y. Petroff, and M. Balkanski, Phys. Rev. 1, 2661 (1970).
[25]Y. W. Tung and M. L. Cohen, Phys. Rev. 180, 823 (1969).
[26]A. O. E. Animalu and V. Heine, Philos. Mag. 12, 1249 (1965).
[27]D. R. Penn, Phys. Rev. 128, 2093 (1962).
[28]F. Hulliger and E. Mooser, *Progress in Solid State Chemistry* (Pergamon, Oxford, England, 1965), Vol. 2.
[29]F. Bassani and M. Schlüter (unpublished).
[30]F. Herman and S. Skillman, *Atomic Structure Calculations* (Prentice-Hall, Englewood Cliffs, N. J., 1963).
[31]G. Harbecke, F. Bassani, and E. Tosatti, in *Proceedings of the Eleventh International Conference on the Physics of Semiconductors*, 1972 (Polish Scientific Publishers, Warsaw, 1972).
[32]Ch. Depeursinge (private communication).
[33]A. J. Grant and A. D. Yotte, Phys. Status Solidi 43, K29 (1971).

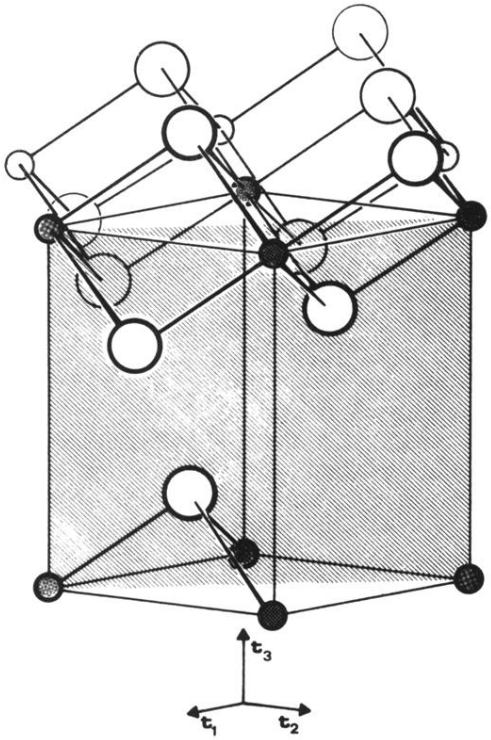

FIG. 1. Perspective view of the atomic positions in PbI_2. The large circles mark the iodine atoms, the small shaded circles represent the lead atoms. The (110) plane is indicated.

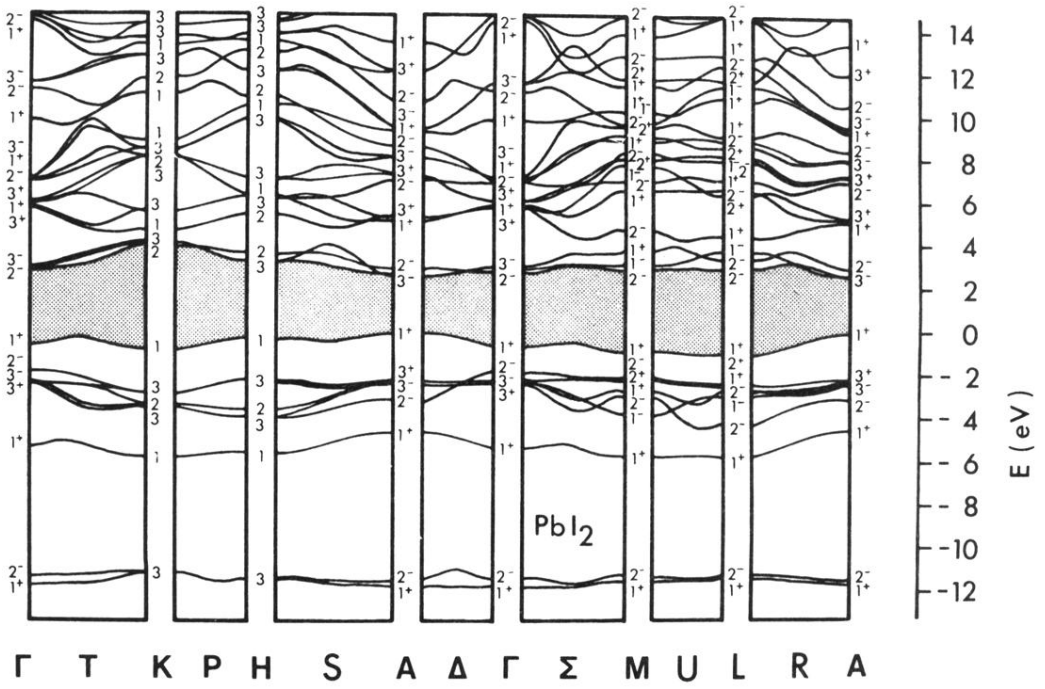

FIG. 3. Band Structure of PbI_2 along high-symmetry lines in the hexagonal Brillouin zone.